IEEE Access
Multidisciplinary | Rapid Review | Open Access Journal

Received July 26, 2021, accepted August 21, 2021, date of publication September 10, 2021, date of current version September 28, 2021.

Digital Object Identifier 10.1109/ACCESS.2021.3111916

Performance Analysis of Resource Allocation in THz-Based Subcarrier Index Modulation Systems for Mobile Users

MOHANNAD ALZARD[1], (Student Member, IEEE), SAUD ALTHUNIBAT[2], (Senior Member, IEEE), KENTA UMEBAYASHI[3], (Member, IEEE), AND NIZAR ZORBA[1], (Senior Member, IEEE)

[1]Department of Electrical Engineering, Qatar University, Doha, Qatar
[2]Department of Communications Engineering, Al-Hussein Bin Talal University, Ma'an 71111, Jordan
[3]Department of Electrical and Electronic Engineering, Tokyo University of Agriculture and Technology, Fuchu, Tokyo 183-8538, Japan

Corresponding author: Nizar Zorba (nizarz@qu.edu.qa)

This work was supported by Qatar University-Marubeni Grant M-QJRC-2020-4. Open Access funding provided by the Qatar National Library.

ABSTRACT The recent demand for connections to a huge number of users with very high data rates have motivated research communities to investigate communications into the higher frequency bands, such as millimeter waves and TeraHertz (THz) bands. Moreover, Subcarrier Index Modulation (SIM) has recently received a significant research efforts analyzing its different performance aspects. In this paper, we propose a SIM system operating over the THz band and analyze its performance considering mobile users and different resource allocation schemes. Specifically, Random WayPoint (RWP) mobility model is considered for users' mobility with different numbers of mobility dimensions, and three different spectrum resource allocation schemes, namely, fixed-order allocation, random allocation and distance-aware allocation are considered. Our analysis includes deriving mathematical expressions of both the average Bit Error Rate (BER) and the average Outage Probability (OP) for the three resource allocation schemes. Simulation results analyze different performance metrics like the BER and the OP and are shown to validate the accuracy of the derived expressions.

INDEX TERMS Terahertz band, index modulation, subcarrier index modulation, resource allocation.

I. INTRODUCTION

Aiming at accommodate the increasing demands on the spectrum resources to satisfy higher data rates, research communities have been exploring the jump to higher frequency bands such as millimeter waves and TeraHertz bands (THz) [1]. These frequency bands afford extremely high data rates and accommodate a huge number of users for recent applications such as Internet of Things (IoT), where huge number of devices are simultaneously connected [2]. However, these frequency bands are severely impacted by the propagation loss, therefore they are mainly exploited for short-range applications in indoor environments with Line-of-Sight (LoS) communication [3].

The associate editor coordinating the review of this manuscript and approving it for publication was Yufeng Wang.

THz band has been under investigation lately in many literature works. In [4], the average interference power and outage probability in THz band (0.1-1 THz) have been analyzed using stochastic geometry, while in [5], 300 GHz channel is modeled considering both time and frequency domains characteristics. In another work, a new two-dimensional geometric model is proposed in [6] for short range device to device (D2D) channels. In [7], a multiple input multiple output (MIMO) channel model is proposed for THz frequency band to increase the communication distance by beamforming and increasing the communication capacity by spatial multiplexing, which have been shown to improve the Signal to Interference and Noise Ratio (SINR) for THz communication systems. In [8], a distance-aware multicarrier modulation is presented to utilize the THz band distance dependency to improve the transmission distance. In [9], a hierarchical modulation scheme is proposed in THz band, making use of

the highly distance-dependent channel in THz band. The first standardization efforts in sub-THz band, IEEE 802.15.3d, have been described in [10] along with initial performance evaluation results. In [11], massive MIMO is suggested for overcoming the pathloss issue in THz band communication where the molecular absorption in Line-of-Sight (LoS) communication can be re-radiated to provide multiple scattering paths to increase the diversity gain in massive MIMO systems. Recently, motivated by the extremely short wavelengths in THz, which allows to install hundreds of nano-antennas, spatial modulation is suggested for the THz band in [12].

A significant portion of research efforts in THz band has been directed to propose different resource allocation schemes for either maximizing data rate, minimizing energy consumption or maximizing communication distance. In [13], a resource allocation scheme is developed for the THz band to maximize the communication distance strategically by utilizing the distance and the bandwidth relationship to distribute spectrum sub-windows, allocate transmit power and select modulation. In [14], a Quality of service (QoS)-aware bandwidth allocation is proposed for THz backhaul network to ensure QoS requirements are satisfied, in terms of higher network throughput and more successful scheduled flows of data. In [15], a non-orthogonal multiple access system is used in the THz band, where energy efficiency optimization is considered, and the Dinkelback-style algorithm is utilized to solve the problem for power optimization and resource allocation. Moreover, energy-efficient resource allocation techniques have been an interesting topic in literature for the past couple of years, in [16]–[18] different resource allocation strategies were discussed for LTE based communication systems.

Multi-carrier modulation has become a key technology since the evolving of 3G, where it has been included in many wireless standards. This is due to the fact it has been nominated an effective solution to cancel the intersymbol interference in the frequency selective channels. Moreover, the increase need for high data rates has allowed the development of several basic multi-carrier modulation techniques. One of the promising multi-carrier modulation systems is the so called Sub-carrier Index Modulation (SIM) [19] that represents a smart reflection of the Index Modulation (IM) concept [20] on the multi-carrier systems. The IM concept implies that part of a data block can be conveyed by activating a subset of the available transmission entities at the transmitter. A transmission entity can be either an antenna, a frequency sub-carrier or a time slot. IM has been widely applied into different communication scenarios and applications due to its promising features in spectral and energy efficiencies [21]. As for SIM, the total spectrum bandwidth is divided into windows, where each window includes a set of sub-carriers. A user that is scheduled on a window will divide its transmitted data block into two parts. The first part is conventionally modulated, while the second determines the index of a subset of the sub-carriers to be used for transmitting the modulated symbol.

SIM has received a high attention and several SIM variants have been proposed in the literature [21]–[24]. Also, its performance has been evaluated considering different scenarios, channel conditions and network topology. SIM showed interesting performance in GHz band in literature and to the best of our knowledge, the performance analysis of SIM in THz band has not been conducted yet. Therefore, aiming at elaborating on the SIM performance analysis, a THz-based SIM systems is proposed and its performance analysis considering mobile users is addressed. Specifically, the average bit error rate (BER) at a set of mobile users being served via a THz-based SIM system is mathematically analyzed. The mobility model adopted to emulate the users mobility is the well-known Random WayPoint (RWP) model [25]–[27], while the well-known different spectrum resource allocation schemes have been considered including fixed, random and distance-aware resource allocation schemes to analyze the BER and the outage probability, therefore, the considered allocation schemes have no constraints. The contributions of this work can be summarized as follows:

- For the first time, THz-based SIM system is proposed and analyzed considering mobile users.
- The average BER at stationary users in THz-based SIM system is derived in a closed form expression.
- The average BER at mobile users in THz-based SIM system is derived in a closed form expression for three different allocation schemes.
- The outage probability at mobile users in THz-based SIM system is derived for the three resource allocation schemes.
- Evaluating the performance of THz-based SIM systems considering three resource allocation schemes in terms of BER and outage probability.

Moreover, all the derived BER closed form expressions (without the molecular absorption factor [28]) have been compared to Monte Carlo simulations (with the molecular absorption consideration), showing a marginal effect of the molecular absorption within practical SNR range, and standing as an upper bound to the actual performance.

The rest of this paper is organized as follows. In Section II, the system model is presented along with an overview of SIM system and RWP mobility model. The considered resource allocation schemes that are tackled in this paper, are briefly described in Section III. In Section IV, performance analysis is conducted and closed form expressions of the average BER are derived. In Section V the mathematical representations for the outage probability in SIM systems are derived. Finally, derived formulas are validated by simulation results in Section VI and conclusions are drawn in Section VII.

II. SYSTEM MODEL

The considered system consists of a set of N users to be served over a portion of the THz band $[1 - 1.15]$ THz, and by a single Base Station (BS). The system is being operated by a single operator model, since for systems working over the THz band, the interference caused by multiple operators

is negligible due to the short-range constraint on THz communication. To this end, the considered band is divided into spectrum windows, where each window includes identical number of subcarriers. Without loss of generality, the number of spectrum windows is equal to the number of users (i.e. N), and the number of subcarriers per window is set to L.

In THz frequency band, the signal is subject to spreading attenuation and the attenuation due to the molecular absorption, therefore in this paper a THz-based LoS channel model is used, which is expressed as follows [11, eq. 8], [12].

$$h_{n,l,w} = \left(\frac{\sqrt{G_t}\,\sqrt{G_r}\,c}{4\pi\, f_{l,w}\, r_n}\right) e^{-k(f_{l,w})\frac{r_n}{2}} \times e^{j2\pi\frac{r_n}{\lambda}} \tag{1}$$

where $h_{n,l,w}$ is the channel transfer function of user n ($n = 1, 2, \ldots, N$) over the ℓ^{th} subcarrier ($\ell = 1, 2, \ldots, L$) in the window w ($w = 1, 2, \ldots, N$), $f_{l,w}$ is the subcarrier frequency, r_n is the distance from the BS to the user, $k(f_{l,w})$ is the molecular absorption coefficient of subcarrier ℓ in window w, λ is the wavelength, c is the speed of light and G_t, G_r are the transmitter and receiver antenna gains, respectively.

The users are assumed to be mobile in the system model. Therefore, we adopt the well-known (RWP) mobility model [26] to describe the users' mobility. RWP model implies that the user is moving within an area whose center is the BS, and its distance r_n varies within the range $[0, R]$, where R is the maximum distance. Different movement space geometries can be considered in the RWP model including the one-dimensional (line), two-dimensional (circle), or three-dimensional (sphere). Being a random variable, the instantaneous value of d_n has a probability density function, $f_r(r_n)$, given as [29], [30]

$$f_r(r_n) = \sum_{i=1}^{\mu} \eta_i R^{-\epsilon_i - 1} r_n^{\epsilon_i}, \tag{2}$$

where μ, ϵ_i and η_i are parameters that depend on the specific movement geometry, as listed in Table 1 [29]. The CDF can be expressed as follows

$$F_r(r_n) = \begin{cases} \dfrac{3r_n^2}{R^2} - \dfrac{2r_n^3}{R^3}, & \text{1D} \\ \dfrac{12}{73}\left(\dfrac{27r_n^2}{2R^2} - \dfrac{35r_n^4}{4R^4} + \dfrac{8r_n^6}{6R^6}\right), & \text{2D} \\ \dfrac{35}{72}\left(\dfrac{7r_n^3}{R^3} - \dfrac{34r_n^5}{5R^5} + \dfrac{13r_n^7}{7R^7}\right), & \text{3D} \end{cases} \tag{3}$$

TABLE 1. Movement area settings [29].

Movement space	μ	η_i	ϵ_i
1D	2	$[6, -6]$	$[1, 2]$
2D	3	$\frac{12}{73}[27, -35, 8]$	$[1, 3, 5]$
3D	3	$\frac{35}{72}[21, -34, 13]$	$[2, 4, 6]$

A. SUBCARRIER INDEX MODULATION OVERVIEW

SIM implies that each user is allocated a spectrum window to transmit its own data. Data are divided into blocks where each block includes $B = \lfloor \log_2 \binom{L}{La} \rfloor + \log_2 M$ bits where M is the modulation order, and $1 \leq L_a < L$ is the number of active subcarriers per window. Each block is further divided into two parts, namely, modulation bits and index selection bits. The modulation bits are passed through the conventional signal modulator to generate a complex-value modulated symbol, while the other part, i.e. index bits, are used to select the index of the subset of the subcarriers to be activated for transmitting the modulated symbol.

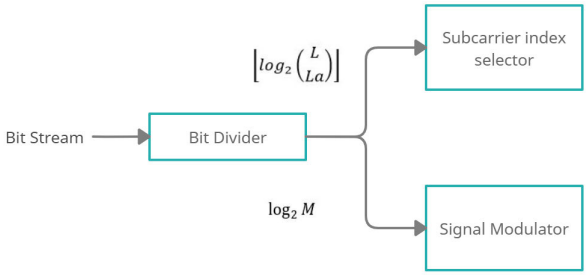

FIGURE 1. Illustration of the Sub Carrier index modulation bit splitting.

In Fig. 1, the bit block splitting in SIM system is depicted, where the first $\lfloor \log_2 \binom{L}{La} \rfloor$ bits are used to select the active subcarrier(s) that will be used to transmit the modulated symbol from the remaining $\log_2 M$ bits in the transmitted block.

Following SIM principles, if the window w is assigned to the user n, the transmitted vector from the user n, denoted by $\boldsymbol{x}_{n,w}$, will include L elements, where its ℓ^{th} element is denoted by $x_{n,w,\ell}$ and given as

$$x_{n,w,\ell} = \begin{cases} 0, \text{ if } \ell \notin A \\ s_n, \text{ if } \ell \in A \end{cases}, \tag{4}$$

where s_n is the modulated symbol of the user n, and A is the selected subset of the subcarriers.

The received signal at the BS from the user n over the window w can be formulated as follows

$$\boldsymbol{y}_{n,w} = \sqrt{P_t}\, \boldsymbol{h}_{n,w} \odot \boldsymbol{x}_{n,w} + \boldsymbol{z}_w, \tag{5}$$

where $\odot$ is the element wise product and P_t is the transmit power, $\boldsymbol{h}_{n,w}$ is the channel vector and $\boldsymbol{z}_w$ is the added complex white Gaussian noise vector at the receiver and N_0 is its power.

To detect the signal and retrieve the transmitted block, Maximum Likelihood (ML) detector is applied at the receiver as follow

$$\hat{\boldsymbol{x}}_{n,w} = \arg \min_{i=1,\ldots,2^B} \left| y_{n,w} - \sqrt{P_t}\boldsymbol{h}_{n,w} \odot \boldsymbol{x}^{(i)} \right|^2 \tag{6}$$

where $\boldsymbol{x}^{(i)}$ ($1 \leq i \leq 2^B$) represents the set of the potential transmitted vectors.

III. RESOURCE ALLOCATION

Resource allocation schemes have a significant impact on the per-user or overall performance. To this end, three

different well-known resource allocation are considered to analyze their performance in THz-based SIM systems in the next section. The considered resource allocation schemes are briefly described as follows

1) Fixed-Order Resource Allocation: where a specific allocation order is assumed, and windows are assigned based on it. Specifically, the user whose order is the first will occupy the lowest spectrum window (the best window). Such a scheme is widely adopted when users are prioritized based on their QoS requirements.
2) Random Resource Allocation: in this scheme, the spectrum windows are randomly assigned to different users regardless of any related metric. Since the number of users is assumed to be identical to the number of windows, each user will be allocated a single spectrum window.
3) Distance-aware Resource Allocation: in this scheme, users are served based on their distance from the BS, where the nearest user will occupy the lowest spectrum window. Such a scheme follows an opportunistic approach aiming at improving the overall system performance.

IV. BER ANALYSIS

This section is mainly dedicated for analyzing the performance in terms of the average BER which will be derived using the union bounding techniques.

Due to the frequency band used in this paper [1−1.15] THz and the maximum communication distance of 10m, the attenuation due to molecular absorption is $\approx$ 1, therefore the channel magnitude of the channel model in (1) is simplified as follows

$$|h_{n,\ell,w}|^2 \approx \frac{G_t\, G_r\, c^2}{(4\pi)^2 f_{\ell,w}^2\, r_n^2} \tag{7}$$

where $h_{n,\ell,w}$ represents the path loss experienced by the signal from the user n over the ℓ^{th} subcarrier in the window w.

The received signal can be formulated as follows

$$\boldsymbol{y}_{n,w} = \sqrt{P_t}\boldsymbol{t}_{n,w} \odot \boldsymbol{x}_{n,w} + z_w, \tag{8}$$

where $\boldsymbol{t}_{n,w}$ is an $L \times 1$ vector whose ℓ^{th} element is equal to $\sqrt{|h_{n,\ell,w}|^2}$.

Similarly, Maximum Likelihood (ML) detector is applied at the receiver as follow

$$\hat{\boldsymbol{x}}_{n,w} = \arg \min_{i=1,\ldots,2^B} \left| \boldsymbol{y}_{n,w} - \sqrt{P_t}\boldsymbol{t}_{n,w} \odot \boldsymbol{x}^{(i)} \right|^2 \tag{9}$$

In Fig. 2 the relationship between distance, frequency and pathloss is shown where it shows how THz frequency band is highly dependent on distance.

A. BER AT STATIONARY USERS WITH FIXED-ORDER ALLOCATION

In this scenario, it is assumed that the window w is always allocated to user n who is assumed to be stationary.

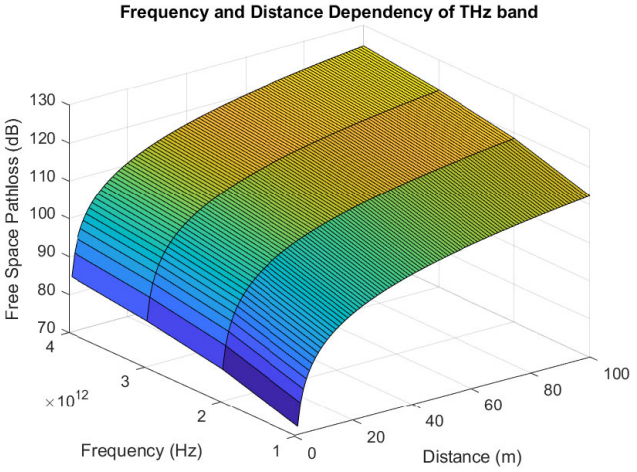

FIGURE 2. Illustration of free space pathloss in THz frequency band.

Therefore, the average BER can be generally formulated using the union bounding technique as follows [31]

$$\text{BER} = \frac{1}{B2^B} \sum_{p=1}^{2^B} \sum_{q=1}^{2^B} \delta_{p,q} \text{PEP}_{p,q}, \tag{10}$$

where $\text{PEP}_{p,q}$ is the pairwise error probability that the vector $\boldsymbol{x}^{(q)}$ is detected given that $\boldsymbol{x}^{(p)}$ is actually transmitted, B is the number of bits in each block and $\delta_{p,q}$ is the number of different bits between the corresponding bit blocks of both $\boldsymbol{x}^{(q)}$ and $\boldsymbol{x}^{(p)}$.

According to its definition and based on (9), $\text{PEP}_{p,q}$ can be expressed as follows:

$$\begin{aligned} \text{PEP}_{p,q} = \text{Pr.}\Big\{ &\left| \boldsymbol{y}_{n,w} - \sqrt{P_t}\boldsymbol{t}_{n,w} \odot \boldsymbol{x}^{(p)} \right|^2 \\ &> \left| \boldsymbol{y}_{n,w} - \sqrt{P_t}\boldsymbol{t}_{n,w} \odot \boldsymbol{x}^{(q)} \right|^2 \Big\} \end{aligned} \tag{11}$$

where Pr. is the probability. Recall that $\boldsymbol{x}^{(p)}$ is the transmitted vector, and hence, $\text{PEP}_{p,q}$ can be simplified as

$$\text{PEP}_{p,q} = \text{Pr.}\left\{ |z_w|^2 > \left| \sqrt{P_t}\boldsymbol{t}_{n,w} \odot \boldsymbol{\Delta}^{(pq)} + z_w \right|^2 \right\}, \tag{12}$$

with $\boldsymbol{\Delta}^{(pq)} = \boldsymbol{x}^{(p)} - \boldsymbol{x}^{(q)}$. (12) can be expressed in terms of the Q-function to yield

$$\text{PEP}_{p,q} = Q\left(\sqrt{\frac{P_t \left| \boldsymbol{t}_{n,w} \odot \boldsymbol{\Delta}^{(pq)} \right|^2}{2\sigma^2}} \right) \tag{13}$$

where σ^2 is the noise variance.

B. BER AT MOBILE USERS WITH FIXED-ORDER ALLOCATION

In the case of mobile users, the pairwise error probability $\text{PEP}_{p,q}$ obtained in (13) should be integrated over the pdf of

the distance given in (2), as follows

$$\mathrm{PEP}_{p,q} = \sum_{i=1}^{\mu} \eta_i R^{-\epsilon_i - 1} \times \int_0^R Q\left(\sqrt{\frac{P_t \left|\boldsymbol{t}_{n,w} \odot \boldsymbol{\Delta}^{(pq)}\right|^2}{2\sigma^2}}\right) \times r_n^{\epsilon_i} \cdot dr_n \tag{14}$$

where ϵ_i is a mobility parameter defined in (2). Equation (14) can be rewritten using the complementary error function as follows $\left(Q(\sqrt{a}) = \frac{1}{2}\mathrm{erfc}(\sqrt{a/2})\right)$

$$\mathrm{PEP}_{p,q} = \sum_{i=1}^{\mu} \frac{\eta_i R^{-\epsilon_i - 1}}{2} \times \int_0^R \mathrm{erfc}\left(\sqrt{\frac{P_t \left|\boldsymbol{k}_{n,w} \odot \boldsymbol{\Delta}^{(pq)}\right|^2}{4\, r_n^2\, \sigma^2}}\right) \times r_n^{\epsilon_i} \cdot dr_n \tag{15}$$

where $\boldsymbol{k}_{n,w} = r_n \boldsymbol{t}_{n,w}$. Now, using [33, eq. 8.4.14.2], the erfc in (16) can be replaced by the Meijer-G function to yield

$$\mathrm{PEP}_{p,q} = \sum_{i=1}^{\mu} \frac{\eta_i R^{-\epsilon_i - 1}}{2\sqrt{\pi}} \int_0^R r_n^{\epsilon_i} G_{1,2}^{2,0}\left(\rho\, r_n^{-2} \middle| \begin{matrix} 1 \\ 0, \frac{1}{2} \end{matrix}\right) \cdot dr_n \tag{16}$$

where $\rho = \frac{P_t \left|\boldsymbol{k}_{n,w} \odot \boldsymbol{\Delta}^{(pq)}\right|^2}{4\sigma^2}$. Eqn. (16) can be solved using [33, eq. 2.24.2.3] to yield

$$\mathrm{PEP}_{pq} = \sum_{i=1}^{\mu} \frac{\eta_i}{4\sqrt{\pi}} G_{2,3}^{3,0}\left(\rho R^{-2} \middle| \begin{matrix} 1, \frac{\epsilon_i+3}{2} \\ \frac{\epsilon_i+3}{2}, 0, \frac{1}{2} \end{matrix}\right). \tag{17}$$

Finally, (17) is substituted in (10) to get the average BER of the mobile user n over the window w according to fixed-order allocation scheme as follows

$$\mathrm{BER}_{n,w}^{\mathrm{Fixed}} = \frac{1}{B2^B} \sum_{p=1}^{2^B} \sum_{q=1}^{2^B} \sum_{i=1}^{\mu} \frac{\delta_{p,q}\eta_i}{4\sqrt{\pi}} G_{2,3}^{3,0}\left(\rho R^{-2} \middle| \begin{matrix} 1, \frac{\epsilon_i+3}{2} \\ \frac{\epsilon_i+1}{2}, 0, \frac{1}{2} \end{matrix}\right). \tag{18}$$

C. BER AT MOBILE USERS WITH VARIABLE ALLOCATION

1) RANDOM ALLOCATION

In the case of random resource allocation, each window will be randomly allocated to the users. Thus, the probability that a user will be scheduled to the window w is identical for all users and equal to $\frac{1}{N}$. As such, the average BER of the mobile user n considering the random allocation is given as follows

$$\mathrm{BER}_n^{\mathrm{Random}} = \frac{1}{N} \sum_{w=1}^{N} \mathrm{BER}_{n,w}^{\mathrm{Fixed}} \tag{19}$$

where $\mathrm{BER}_{n,w}^{\mathrm{Fixed}}$ can be substituted from (18) to yield

$$\mathrm{BER}_n^{\mathrm{Random}} = \frac{1}{N\, B2^B} \sum_{w=1}^{N} \sum_{p=1}^{2^B} \sum_{q=1}^{2^B} \sum_{i=1}^{\mu} \frac{\delta_{p,q}\eta_i}{4\sqrt{\pi}} \times G_{2,3}^{3,0}\left(\rho R^{-2} \middle| \begin{matrix} 1, \frac{\epsilon_i+3}{2} \\ \frac{\epsilon_i+1}{2}, 0, \frac{1}{2} \end{matrix}\right) \tag{20}$$

2) DISTANCE-AWARE ALLOCATION

Due to the fact that the distance-aware allocation is based mainly on the distance, where the nearest user gets the lowest spectrum window, the derivation of the average BER of any of the users differs from the previous cases. In general, the average BER of the mobile user n according to the distance-aware resource allocation can be formulated as follows

$$\mathrm{BER}_n^{\text{distance-aware}} = \sum_{i=1}^{N} \Pr.(\tau_n = i) \mathrm{BER}_n^{\tau_n = i} \tag{21}$$

where τ_n represents the distance order of the user n ($1 \leq \tau_n \leq N$), $\Pr.(\tau_n = i)$ is the probability that $\tau_n = i$, and $\mathrm{BER}_n^{\tau_n=i}$ is the average BER of the user n when $\tau_n = i$ according to the distance-aware allocation. Since all users have identical mobility model, $\Pr.(\tau_n = i)$ is equal to $\frac{1}{N}$ for all i and n values, which makes (21) rewritten as

$$\mathrm{BER}_n^{\text{distance-aware}} = \frac{1}{N} \sum_{i=1}^{N} \mathrm{BER}_n^{\tau_n = i} \tag{22}$$

Now, from its definition, $\mathrm{BER}_n^{\tau_n=i}$ can be expressed as follows

$$\mathrm{BER}_n^{\tau_n=i} = \frac{1}{B2^B} \sum_{p=1}^{2^B} \sum_{q=1}^{2^B} \delta_{p,q} \mathrm{PEP}_{p,q}^{\tau_n=i}, \tag{23}$$

where $\mathrm{PEP}_{p,q}^{\tau_n=i}$ can be expressed by the aid of (13) as follows

$$\mathrm{PEP}_{p,q}^{\tau_n=i} = \frac{1}{2\sqrt{\pi}} \int_0^R G_{1,2}^{2,0}\left(\rho\, \hat{r}_i^{-2} \middle| \begin{matrix} 1 \\ 0, \frac{1}{2} \end{matrix}\right) f_{\hat{r}_i}(\hat{r}_i) \cdot d\hat{r}_i \tag{24}$$

where $f_i(r_n)$ is the pdf of the i^{th} maximum distance which can be expressed using the order statistics theory as follows:

$$f_i(r_n) = \frac{N!}{(i-1)!(N-i)!} f_r(r_n) \left(F_r(r_n)\right)^{i-1} \times \left(1 - F_r(r_n)\right)^{N-i} \tag{25}$$

Now substituting (3) and (25) in (24), the pairwise error probability can be solved using binomial expansion. [35, eqs. 5.3 & 5.12] and [33, eq. 2.24.2.3] to yield (26), (27) and (28), as shown at the bottom of the next page, for the cases of 1D, 2D and 3D, respectively, where ζ_{1D}, ζ_{2D}, ζ_{3D}, A_{1D}, A_{2D}, and A_{3D}, as shown at the bottom of the next page.

Finally, the corresponding average BER formulas can be obtained by substituting (26)-(28) into (23) and then into (22).

V. OUTAGE PROBABILITY ANALYSIS

In this section, outage probability [34] of THz-based SIM system is analyzed for mobile users considering different resource allocations schemes. Generally, the outage probability is defined as the probability that the operating SNR is less than a preset threshold (γ). Accounting for the windows allocation and the subcarrier activation in SIM systems, the outage probability can be expressed as:

$$P_{\mathrm{out}}(n) = \sum_{w=1}^{N} \Pr.(w) \sum_{\ell=1}^{L} \Pr.(\ell)\, \Pr.(\mathrm{SNR}_{n,\ell} < \gamma), \tag{29}$$

where $\Pr.(w)$ is the probability that user n will be scheduled to operate over the window w, $\Pr.(\ell)$ is the probability that the subcarrier ℓ is activated, and $\Pr.(\text{SNR}_{n,\ell} < \gamma)$ is the probability that SNR of the user n over the subcarrier ℓ is less than the threshold (γ).

The probability $\Pr.(\ell)$ is actually identical for all schemes and for all subcarriers in a window and equals to $\Pr.(\ell) = \frac{1}{L}$. However the probability $\Pr.(w)$ is different for each resource allocation technique, as will be discussed later. Also, the $\text{SNR}_{n,\ell}$ is expressed as follows

$$\text{SNR}_{n,\ell} = \frac{P_t\, G_t\, G_r\, c^2}{(4\pi)^2 f_{\ell,w}^2\, r_n\, N_o}\, e^{-k[f_{\ell,w}]\times r_n}. \tag{30}$$

However given the frequency band considered and communication distance assumed in this paper, the exponential term (i.e., attenuation due to the molecular absorption) can be neglected as it is approximately approaches unity (i.e., $e^{-k[f_{\ell,w}]\times r_n} \approx 1$. Therefore, the SNR expression given in (30) can be approximated as follows

$$\text{SNR}_{n,\ell} \approx \frac{P_t\, G_t\, G_r\, c^2}{(4\pi)^2 f_{\ell,w}^2\, r_n\, N_o} \tag{31}$$

It should be noted that (based on (31)) the only variable parameter in the SNR calculation is the user distance r_n. Therefore, the probability $\Pr.(\text{SNR}_{n,\ell} < \gamma)$ can be represented with respect to the user distance as follows

$$\Pr.(\text{SNR}_{n,\ell} < \gamma) = \Pr.(r_n > \Gamma_{n,w,\ell}) \tag{32}$$

where $\Gamma_{n,w,\ell}$ is given as follows

$$\Gamma_{n,w,\ell} = \frac{P_t\, G_t\, G_r\, c^2}{\gamma\, N_o\, (4\pi)^2 f_{\ell,w}^2} \tag{33}$$

Hence, the outage probability can be rewritten as:

$$P_{\text{out}}(n) = \frac{1}{L}\sum_{w=1}^{N} \Pr.(w) \sum_{\ell=1}^{L} \Pr.(r_n > \Gamma_{n,w,\ell}) \tag{34}$$

A. FIXED-ORDER RESOURCE ALLOCATION

In the fixed-order allocation scheme, the windows allocation is fixed where each user is always allocated to the same spectrum window. By denoting the allocated window to user n by w_n, $\Pr.(w)$ for fixed-order alocation scheme is expressed as follows:

$$\Pr.(w)_{(FA)} = \begin{cases} 1 & \text{If } w = w_n \\ 0 & \text{Otherwise.} \end{cases} \tag{35}$$

Moreover, the probability $\Pr.(r_n > \Gamma_{n,w,\ell})$ is calculated by using the RWP-Model CDF in (3) to be $\Pr.(r_n > \Gamma_{n,w,\ell}) = 1 - F_r(\Gamma_{n,w,\ell})$. Finally, the outage probability for the fixed-order allocation scheme can be rewritten as follows

$$P_{\text{out}}(FA) = \frac{1}{L}\sum_{w=1}^{N} Pr(w)_{(FA)} \sum_{l=1}^{L} 1 - F_r(\Gamma_{n,w,\ell}) \tag{36}$$

B. RANDOM RESOURCE ALLOCATION

In the random resource allocation scheme,the probability of user n being assigned to window w is equal-probable (i.e., $\frac{1}{N}$)

$$\begin{aligned}
\zeta_{1D} &= \frac{N!\ (3)^{j+t}\ (2)^{N-k-j-t-1}\ (-1)^{i-1-j}}{(N-i)!\ j!\ k!\ t!\ (i-j-1)!\ (N-i-k-t)!} \\
\zeta_{2D} &= \frac{N!(\frac{12}{73})^{N-t}\ (\frac{27}{2})^{j+b}\ (\frac{35}{4})^{k+b}\ (\frac{8}{6})^{N-j-k-t-a-b}(-1)^{N+k-i-t-b}}{(N-i)!\,j!\,k!\,t!\,(i-1-j-k)!\,a!\,b!\,(N-i-t-a-b)!} \\
\zeta_{3D} &= \frac{N!(\frac{35}{72})^{N-t}\ (\frac{21}{3})^{j+b}\ (\frac{34}{5})^{k+b}\ (\frac{13}{7})^{N-j-k-t-a-b-1}(-1)^{N+k-i-t-b}}{(N-i)!\ j!\,k!\ t!\ (i-1-j-k)!\ a!\ b!\ (N-i-t-a-b)!} \\
A_{1D} &= 3N-3k-t-j-3 \\
A_{2D} &= 6N-6t-4j-2k-2b-4a-6. \\
A_{3D} &= 6N-6t-4j-2k-2b-4a-7.
\end{aligned}$$

$$\text{PEP}_{p,q}^{\tau_n=i} = \sum_{j=0}^{i-1}\sum_{k=0}^{N-i}\sum_{t=0}^{N-i-k} \frac{\zeta_{1D}}{2}\left[G_{2,2}^{3,0}\left(\rho R^{-2}\middle|\begin{matrix}1,\frac{A_{1D}+4}{2}\\ \frac{A_{1D}+2}{2},0,\frac{1}{2}\end{matrix}\right) - G_{2,2}^{3,0}\left(\rho R^{-2}\middle|\begin{matrix}1,\frac{A_{1D}+5}{2}\\ \frac{A_{1D}+3}{2},0,\frac{1}{2}\end{matrix}\right)\right] \tag{26}$$

$$\text{PEP}_{p,q}^{\tau_n=i} = \sum_{j=0}^{i-1}\sum_{k=0}^{i-j-1}\sum_{t=0}^{N-i}\sum_{a=0}^{N-i-t}\sum_{b=0}^{N-i-t-a} \frac{\zeta_{2D}}{3}\left[G_{2,2}^{3,0}\left(\rho R^{-2}\middle|\begin{matrix}1,\frac{A_{2D}+4}{2}\\ \frac{A_{2D}+2}{2},0,\frac{1}{2}\end{matrix}\right) - G_{2,2}^{3,0}\left(\rho R^{-2}\middle|\begin{matrix}1,\frac{A_{2D}+6}{2}\\ \frac{A_{2D}+4}{2},0,\frac{1}{2}\end{matrix}\right) + G_{2,2}^{3,0}\left(\rho R^{-2}\middle|\begin{matrix}1,\frac{A_{2D}+8}{2}\\ \frac{A_{2D}+6}{2},0,\frac{1}{2}\end{matrix}\right)\right] \tag{27}$$

$$\text{PEP}_{p,q}^{\tau_n=i} = \sum_{j=0}^{i-1}\sum_{k=0}^{i-j-1}\sum_{t=0}^{N-i}\sum_{a=0}^{N-i-t}\sum_{b=0}^{N-i-t-a} \frac{\zeta_{3D}}{3}\left[G_{2,2}^{3,0}\left(\rho R^{-2}\middle|\begin{matrix}1,\frac{A_{3D}+5}{2}\\ \frac{A_{2D}+3}{2},0,\frac{1}{2}\end{matrix}\right) - G_{2,2}^{3,0}\left(\rho R^{-2}\middle|\begin{matrix}1,\frac{A_{3D}+7}{2}\\ \frac{A_{3D}+5}{2},0,\frac{1}{2}\end{matrix}\right) + G_{2,2}^{3,0}\left(\rho R^{-2}\middle|\begin{matrix}1,\frac{A_{3D}+9}{2}\\ \frac{A_{3D}+7}{2},0,\frac{1}{2}\end{matrix}\right)\right] \tag{28}$$

due to the assumption that each user will only have a single window. Also, the probability $\Pr.(r_n > \Gamma_{n,w,\ell})$ is calculated by using the RWP-Model CDF in (3) to be $\Pr.(r_n > \Gamma_{n,w,\ell}) = 1 - F_r(\Gamma_{n,w,\ell})$. Therefore, the outage probability for the random allocation scheme is expressed as follows:

$$P_{\text{out}}(RA) = \frac{1}{LN} \sum_{w=1}^{N} \sum_{l=1}^{L} 1 - F_r(\Gamma_{n,w,\ell}) \tag{37}$$

C. DISTANT-AWARE RESOURCE ALLOCATION

In the distance-aware allocation scheme, the windows are allocated to users based on their distances, where the nearest user is allocated the first window (with lowest frequency). As all users have identical mobility model, the probability to be in a specific distance with respect to the others is identical to all users, which implies that $\Pr.(w) = \frac{1}{N}$. As for the probability $\Pr.(r_n > \Gamma_{n,w,\ell})$, it can be obtained by using the order statistics where the CDF of the distance of each distance-order should be obtained. Specifically, following order statistics, the CDF of the k^{th} maximum distance, denoted by $F_{\hat{r}_k}(r)$, is expressed as follows:

$$F_{\hat{r}_k}(r) = \sum_{j=k}^{N} \binom{N}{j} (F_r(r))^j \, (1 - F_r(r))^{N-j}. \tag{38}$$

Finally, the outage probability considering the distance-aware allocation scheme can be expressed as follows:

$$P_{\text{out}}(DA) = \frac{1}{L\,N} \sum_{w=1}^{N} \sum_{l=1}^{L} \sum_{k=1}^{N} 1 - F_{\hat{r}_k}(\Gamma_{n,w,\ell}) \tag{39}$$

VI. SIMULATION RESULTS

In this section, simulation results are explored to validate the mathematical formulas derived in this paper. The LoS channel model in (1) is used in the simulation considering the molecular absorption coefficient $k[f]$ to be approximately $[10^{-2}\ 10^{-3}]$ for the frequency band used. The spectrum band [1 1.15] THz is divided into 16 subcarriers grouped into 4 windows to serve 4 users. However, the system model is valid for any window size value to serve any number of users. The rest of the simulation parameters for BER and outage probability simulations are summarized in Table 2.

TABLE 2. Simulation parameters.

Parameter	Notation	Value
Frequency Band	f	[1 1.15] THz
No. of subcarriers per window	L	4
No. of active subcarriers	La	1
Maximum mobility distance	R	10 meters
Modulation Order	M	4 (QPSK)
Molecular absorption coefficient	$k[f]$	$[10^{-2}\ 10^{-3}]$
Noise Power	N_o	-75 dBW

A. BER RESULTS

In the BER simulation, the gains of the transmit and receive antennas are both set to $G_t = G_r = 10$ dB. All of the

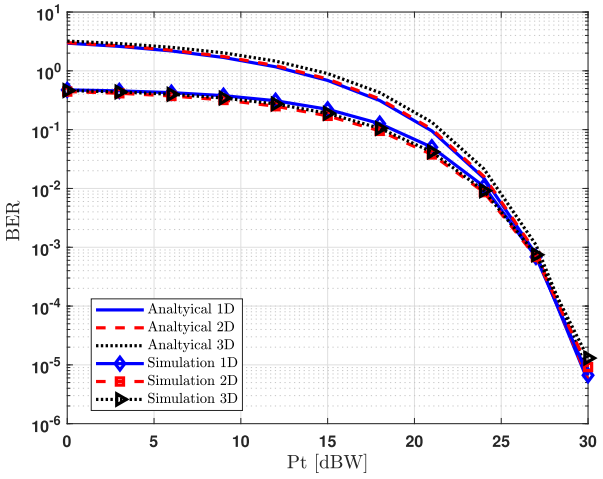

FIGURE 3. The average BER versus P_t in THZ-based SIM system considering the random allocation and the different number of mobility dimensions.

mathematical formulas are derived as an upper bound that approaches the exact simulation results as the transmit power increases. In Fig. 3 and Fig. 4 a comparison between the three different mobility dimensions are plotted where it is clearly shown that the number mobility dimensions has an impact on the overall system performance where an increase of the BER is shown moving from 1D to 3D.

Fig. 3 depicts the average BER versus the transmit power in dBW considering the random resource allocation. As it is a random allocation, the BER at all users is identical, so the BER of only one user is shown. The results show the performance considering different number of mobility dimensions. As clearly shown, the analytical results obtained by (20) provide accurate results which match the simulation results at moderate and high values of P_t. Notice that the obtained analytical BER results is larger than 1 in low P_t values and that is because the analytical BER results represent an upper-bound obtained from the summation of non-complimentary probabilities as shown in (11). The gap between analytical and simulation results at low values of P_t stems from using the union bounding technique in deriving the BER which usually shows such a gap in low values of P_t that diminishes as P_t increases.

In Fig. 4, the distance-aware resource allocation is considered, where the average BER is plotted versus the transmit power at different number of mobility dimensions. As the same distance PDF assumed for all users, the probability that a user be in a specific distance is identical for all users. Thus, their BER curves are identical. As in Fig. 3, the analytical results obtained using (26)-(28) approach the simulation results as P_t increase where an exact matching can be noticed at 20 dBW for the three different numbers of mobility dimensions.

The performance of the fixed-order allocation is considered for 1D, 2D and 3D cases in Fig. 5, Fig. 6 and Fig. 7, respectively. For better visibility, only the BER of the best user (User 1) and the worst user (User 4) are shown in the

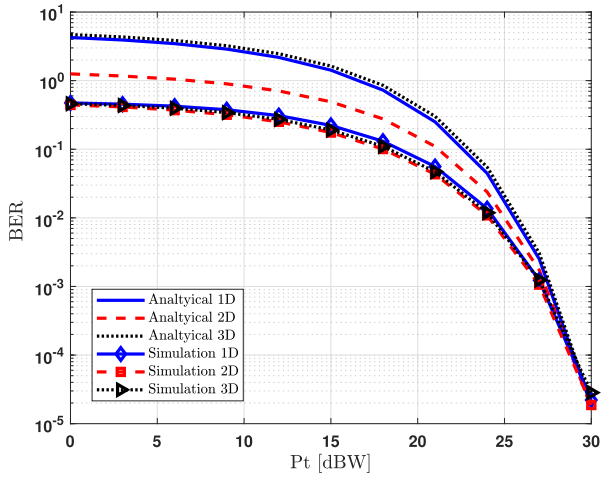

FIGURE 4. The average BER versus P_t in THZ-based SIM system considering the distance-aware allocation and the different number of mobility dimensions.

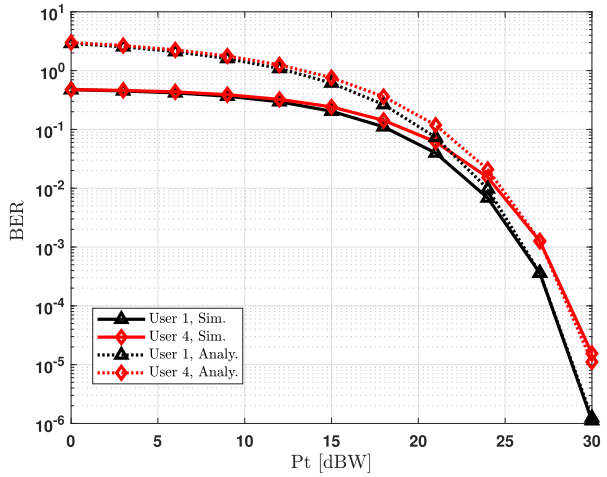

FIGURE 5. The average BER of users 1 and 4 versus P_t in THZ-based SIM system considering the fixed-order allocation for 1D mobility.

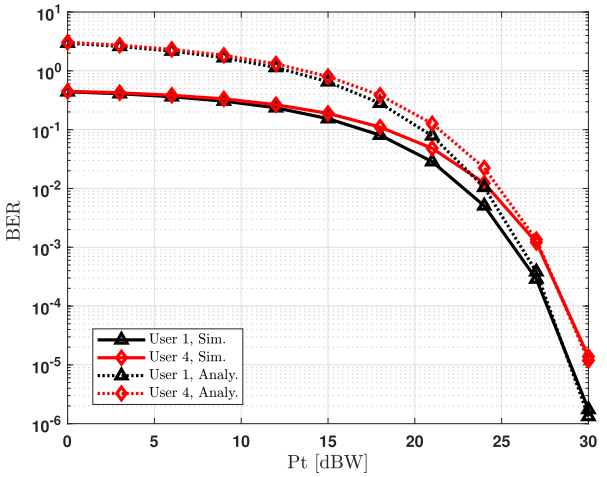

FIGURE 6. The average BER of users 1 and 4 versus P_t in THZ-based SIM system considering the fixed-order allocation for 2D mobility.

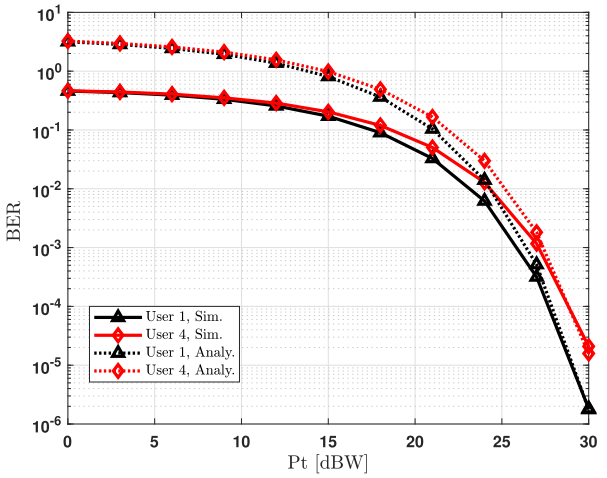

FIGURE 7. The average BER of users 1 and 4 versus P_t in THZ-based SIM system considering the fixed-order allocation for 3D mobility.

figures. As expected, the BER performance of users rely on their order in the resource allocation. User 1 achieves the best BER as it is the first user in resource allocating, while User 4 has the worst performance as it is the last served user. The analytical results obtained by (18) provide a good accuracy compared by the simulation results in the three cases.

In Fig. 8 and Fig. 9, the performance of the three resource allocations are compared at User 1 and User 4, respectively, considering 3D RWP mobility model. Several comments can be made based on these Figures. First, as shown in Fig. 8, the fixed-order allocation is the best option for User 1 since it has the priority to be served before the others. On the other hand, User 4 achieves the best performance when the random allocation is adopted, which is due to the lowest priority given for User 4 (last served). Finally, although it is considered an opportunistic approach, it can be observed that the distance-aware resource allocation attains the worst performance for both users. This is due to the fact that distance-aware allocation can improve the performance and achieves the best BER only if the evaluation is per spectrum window and per user.

B. OUTAGE PROBABILITY RESULTS

In this section the simulation and analytical results for the outage probability are explored and discussed. The simulation parameters are set as in Table 2. However, the transmit antenna gain, receive antenna gain and the transmit power are set to $G_t = 15$ dB, $G_r = 15$ dB and $P_t = 0$ dBW, respectively.

Fig. 10, Fig. 11 and Fig. 12 depict the outage probability for the fixed-order allocation technique versus the SNR threshold γ for 1D, 2D and 3D mobility dimensions, respectively. As shown the outage probability for the first user shows a better performance than the fourth user, and this is due the priority of allocation for the first user.

In Fig. 13 and Fig. 14, the outage probability considering the random allocation scheme and distance-aware scheme is

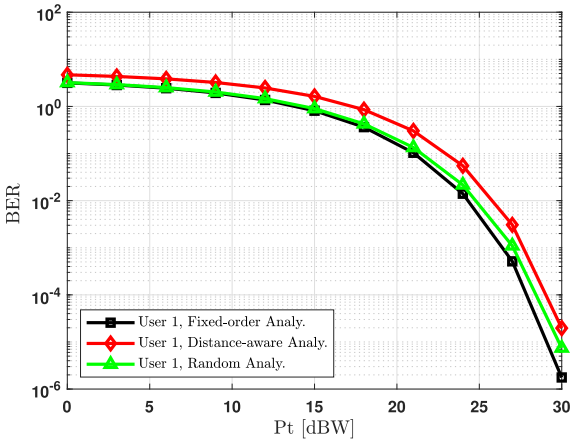

FIGURE 8. BER Comparison of the three considered resource allocation schemes at User 1. 3D mobility is considered.

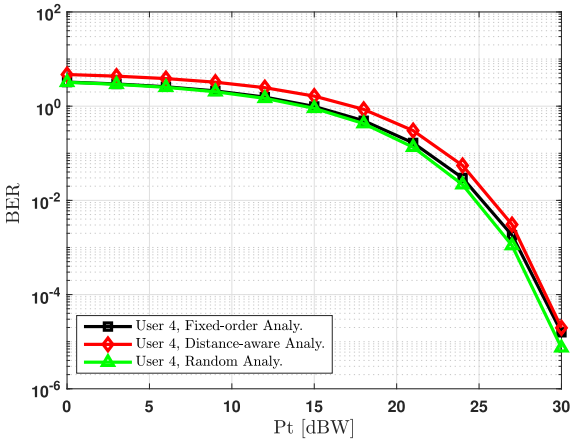

FIGURE 9. BER Comparison of the three considered resource allocation schemes at User 4. 3D mobility is considered.

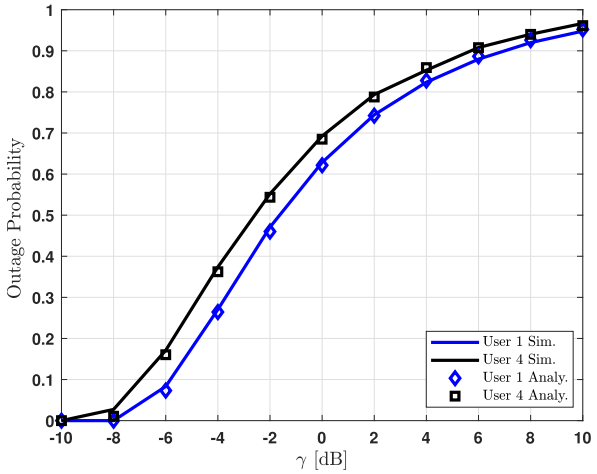

FIGURE 10. The outage probability of users 1 and 4 versus the SNR threshold γ in THZ-based SIM system considering the fixed-order allocation for 1D mobility.

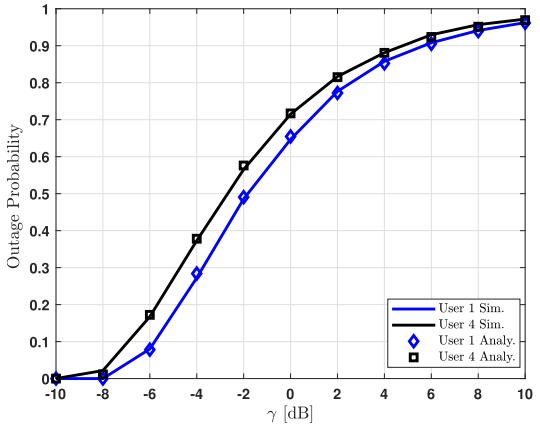

FIGURE 11. The outage probability of users 1 and 4 versus the SNR threshold γ in THZ-based SIM system considering the fixed-order allocation for 2D mobility.

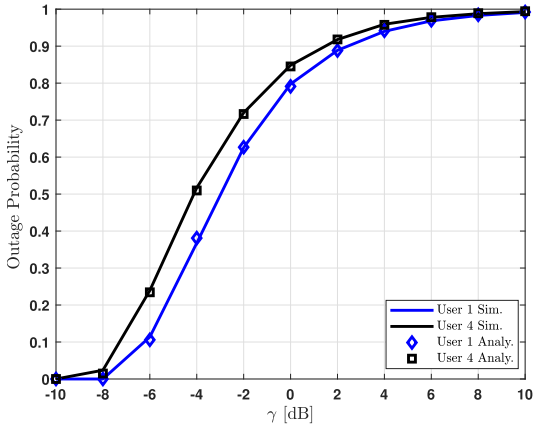

FIGURE 12. The outage probability of users 1 and 4 versus the SNR threshold γ in THZ-based SIM system considering the fixed-order allocation for 3D mobility.

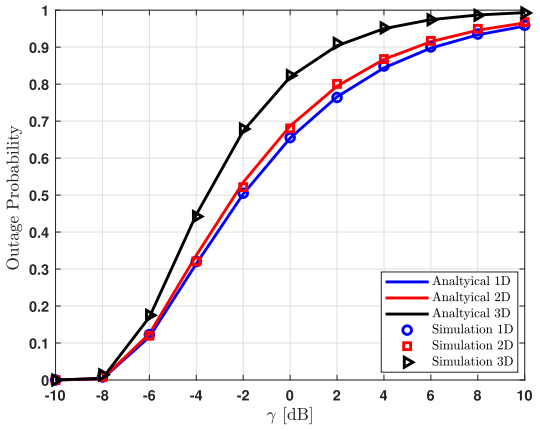

FIGURE 13. The outage probability versus the SNR threshold considering the random resource allocation scheme and different number of mobility dimensions.

shown, respectively, where the performance for the 4 users are identical for both schemes since the probability for the window allocation is $Pr(w) = \frac{1}{N}$ for all users. As clearly shown the analytical (without molecular absorption consideration) and the simulation results (with molecular absorption) are matching at all γ values for the communication distance and the frequency band used in this paper.

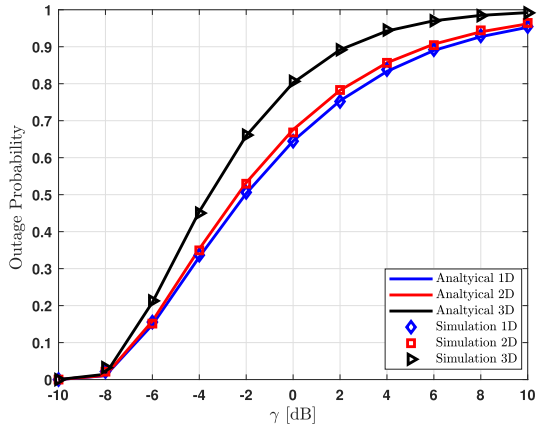

FIGURE 14. The outage probability versus the SNR threshold considering the distance-aware resource allocation scheme and different number of mobility dimensions.

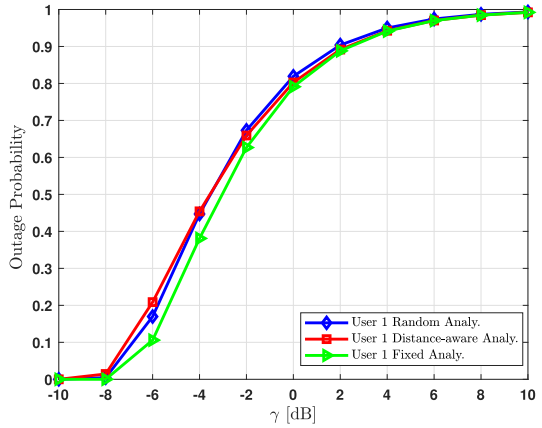

FIGURE 15. Outage probability Comparison for the three considered resource allocation schemes at User 1. 3D mobility is considered.

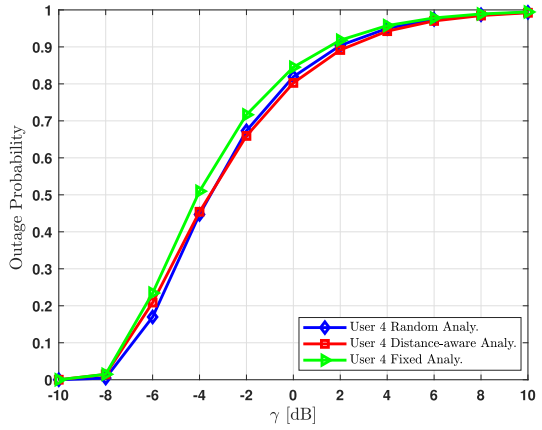

FIGURE 16. Outage probability Comparison for the three considered resource allocation schemes at User 4. 3D mobility is considered.

Finally, in Fig. 15 and Fig. 16, a comparison of the outage probability among the three allocation schemes for User 1 and User 4, respectively. For the fixed-order allocation, it can be noted that the outage performance follows the order of the user. Specifically, for User 1, it provides the best outage performance (lowest outage probability), while for User 4, the highest outage performance is attained by the fixed-order allocation. Comparing the outage performance of the random and distance-aware allocation schemes in both figures, one can clearly observe that the distance-aware allocation provides better outage probability only once the SNR threshold exceeds a specific value. This can be referred to the change in the CDF used and the threshold $\Gamma_{n,w,\ell}$. Specifically, when the threshold value increases the probability that the weighted sum of the ordered distance decreases, which results in a lower outage probability in the distance-aware allocation scheme.

VII. CONCLUSION AND FUTURE WORK

The subcarrier index modulation system is evaluated over the THz frequency band in this paper. Several popular resource allocation schemes have been considered and evaluated for resource allocation in THz-based subcarrier index modulation systems. The average bit error rate is derived for THz-based subcarrier index modulation system considering mobile users. The outage probability closed-form mathematical equations were derived for the THz subcarrier index modulation system. Simulating a LoS THz-based channel with molecular absorption effect showed matching results to the bit error rate and outage probability mathematical expressions derived. In future work, the following points should be explored for further studies on the performance of SIM THz based systems

- Different resource allocation schemes performance optimization for THz based SIM systems.
- Study the effect of multiple operators in THz based SIM systems.
- Proposing a new resource allocation scheme optimized for THz based communication, aimed to improve the bit error rate performance and the communication distance.

ACKNOWLEDGMENT

This work was supported by Qatar University-Marubeni Grant M-QJRC-2020-4. Open Access funding provided by the Qatar National Library.

REFERENCES

[1] K. Rikkinen, P. Kyosti, M. E. Leinonen, M. Berg, and A. Parssinen, "THz radio communication: Link budget analysis toward 6G," *IEEE Commun. Mag.*, vol. 58, no. 11, pp. 22–27, Nov. 2020.
[2] R. Ande, B. Adebisi, M. Hammoudeh, and J. Saleem, "Internet of Things: Evolution and technologies from a security perspective," *Sustain. Cities Soc.*, vol. 54, Mar. 2019, Art. no. 101728.
[3] C. Castro, R. Elschner, T. Merkle, C. Schubert, and R. Freund, "Experimental demonstrations of high-capacity THz-wireless transmission systems for beyond 5G," *IEEE Commun. Mag.*, vol. 58, no. 11, pp. 41–47, Nov. 2020.
[4] J. Kokkoniemi, J. Lehtomäki, and M. Juntti, "Stochastic geometry analysis for mean interference power and outage probability in THz networks," *IEEE Trans. Wireless Commun.*, vol. 16, no. 5, pp. 3017–3028, May 2017.
[5] S. Priebe and T. Kurner, "Stochastic modeling of THz indoor radio channels," *IEEE Trans. Wireless Commun.*, vol. 12, no. 9, pp. 4445–4455, Sep. 2013.
[6] S. Kim and A. Zajić, "Statistical modeling and simulation of short-range device-to-device communication channels at sub-THz frequencies," *IEEE Trans. Wireless Commun.*, vol. 15, no. 9, pp. 6423–6433, Sep. 2016.

[7] X. Lu, M. Lv, T. Hong, and M. Kadoch, "Improvement of SINR for MIMO channels in terahertz communication," in *Proc. Int. Wireless Commun. Mobile Comput. (IWCMC)*, 2020, pp. 489–493.
[8] C. Han and I. F. Akyildiz, "Distance-aware multi-carrier (DAMC) modulation in terahertz band communication," in *Proc. IEEE ICC*, Sydney, NSW, Australia, Jun. 2014, pp. 5461–5467.
[9] Z. Hossain and J. M. Jornet, "Hierarchical bandwidth modulation for ultra-broadband terahertz communications," in *Proc. ICC*, Shanghai, China, 2019, pp. 1–7.
[10] V. Petrov, T. Kurner, and I. Hosako, "IEEE 802.15.3d: First standardization efforts for sub-terahertz band communications toward 6G," *IEEE Commun. Mag.*, vol. 58, no. 11, pp. 28–33, Nov. 2020.
[11] S. A. Hoseini, M. Ding, and M. Hassan, "Massive MIMO performance comparison of beamforming and multiplexing in the terahertz band," in *Proc. IEEE Globecom Workshops (GC Wkshpsop)*, Dec. 2017, pp. 1–6.
[12] H. Sarieddeen, M.-S. Alouini, and T. Y. Al-Naffouri, "Terahertz-band ultra-massive spatial modulation MIMO," *IEEE J. Sel. Areas Commun.*, vol. 37, no. 9, pp. 2040–2052, Jul. 2019.
[13] C. Han and I. F. Akyildiz, "Distance-aware bandwidth-adaptive resource allocation for wireless systems in the terahertz band," *IEEE Trans. THz Sci. Technol.*, vol. 6, no. 4, pp. 541–553, Jul. 2016.
[14] H. Jiang, Y. Niu, B. Ai, Z. Zhong, and S. Mao, "QoS-aware bandwidth allocation and concurrent scheduling for terahertz wireless backhaul networks," *IEEE Access*, vol. 8, pp. 125814–125825, 2020.
[15] H. Zhang, Y. Duan, K. Long, and V. C. M. Leung, "Energy efficient resource allocation in terahertz downlink NOMA systems," *IEEE Trans. Commun.*, vol. 69, no. 2, pp. 1375–1384, Feb. 2021.
[16] D. J. Dechene and A. Shami, "Energy-aware resource allocation strategies for LTE uplink with synchronous HARQ constraints," *IEEE Trans. Mobile Comput.*, vol. 13, no. 2, pp. 422–433, Feb. 2014.
[17] M. Kalil, "Efficient low-complexity scheduler for wireless resource virtualization," *IEEE Wireless Commun. Lett.*, vol. 5, no. 1, pp. 56–59, Feb. 2016.
[18] M. Kalil, A. Shami, A. Al-Dweik, and S. Muhaidat, "Low-complexity power-efficient schedulers for LTE uplink with delay-sensitive traffic," *IEEE Trans. Veh. Technol.*, vol. 64, no. 10, pp. 4551–4564, Oct. 2015.
[19] R. Abu-Alhiga and H. Haas, "Subcarrier-index modulation OFDM," in *Proc. PIMRC*, Tokyo, Japan, 2009, pp. 177–181.
[20] E. Basar, M. Wen, R. Mesleh, M. Di Renzo, Y. Xiao, and H. Haas, "Index modulation techniques for next-generation wireless networks," *IEEE Access*, vol. 5, pp. 16693–16746, 2017, doi: 10.1109/ACCESS.2017.2737528.
[21] E. Başar, U. Aygölü, E. Panayırcı, and H. V. Poor, "Orthogonal frequency division multiplexing with index modulation," *IEEE Trans. Signal Process.*, vol. 61, no. 22, pp. 5536–5549, Nov. 2013.
[22] N. Ishikawa, S. Sugiura, and L. Hanzo, "Subcarrier-index modulation aided OFDM-will it work?" *IEEE Access*, vol. 4, pp. 2580–2593, 2016.
[23] Q. Li, M. Wen, B. Clerckx, S. Mumtaz, A. Al-Dulaimi, and R. Q. Hu, "Subcarrier index modulation for future wireless networks: Principles, applications, and challenges," *IEEE Wireless Commun.*, vol. 27, no. 3, pp. 118–125, Jun. 2020.
[24] S. Althunibat, R. Mesleh, and E. Basar, "Differential subcarrier index modulation," *IEEE Trans. Veh. Technol.*, vol. 67, no. 8, pp. 7429–7436, Aug. 2018.
[25] C. Bettstetter, G. Resta, and P. Santi, "The node distribution of the random waypoint mobility model for wireless ad hoc networks," *IEEE Trans. Mobile Comput.*, vol. 2, no. 3, pp. 257–269, Jul. 2003.
[26] E. Hyytia, P. Lassila, and J. Virtamo, "Spatial node distribution of the random waypoint mobility model with applications," *IEEE Trans. Mobile Comput.*, vol. 5, no. 6, pp. 680–694, Jun. 2006.
[27] S. Althunibat, O. S. Badarneh, and R. Mesleh, "Random waypoint mobility model in space modulation systems," *IEEE Commun. Lett.*, vol. 23, no. 5, pp. 884–887, May 2019.
[28] Z. Wu, H. Ebisawa, J. Lehtomaki, K. Umebayashi, and N. Zorba, "Time domain propagation characteristics with causal channel model for terahertz band," in *Proc. ICC*, May 2021, pp. 1–6.
[29] V. Aalo, C. Mukasa, and G. P. Efthymoglou, "Effect of mobility on the outage and BER performances of digital transmissions over Nakagami-*m* fading channels," *IEEE Trans. Veh. Technol.*, vol. 65, no. 4, pp. 2715–2721, Apr. 2016.
[30] K. Govindan, K. Zeng, and P. Mohapatra, "Probability density of the received power in mobile networks," *IEEE Trans. Wireless Commun.*, vol. 10, no. 11, pp. 3613–3619, Nov. 2001.
[31] J. G. Proakis, *Digital Communications*. New York, NY, USA: McGraw-Hill, 1995.
[32] J. Craig, "A new, simple, and exact result for calculating the probability of error for two-dimensional signal constellations," in *Proc. MILCOM*, 1991, pp. 571–575.
[33] A. P. Prudnikov, *Integrals Series: Russian*, vol. 3. London, U.K.: Taylor & Francis, 1986.
[34] R. Imran, M. Odeh, N. Zorba, and C. Verikoukis, "Quality of experience for spatial cognitive systems within multiple antenna scenarios," *IEEE Trans. Wireless Commun.*, vol. 12, no. 8, pp. 4153–4161, Aug. 2013.
[35] R. M. Graham, D. E. Knuth, and O. Patashnik, *Concrete Mathematics*. Reading, MA, USA: Addison-Wesley, 1994.

MOHANNAD ALZARD (Student Member, IEEE) graduated from the Department of Electrical Engineering, Qatar University, in 2020. He is currently a Research Assistant with Qatar University working on the terahertz technology. His research interests include terahertz communication and wireless systems.

SAUD ALTHUNIBAT (Senior Member, IEEE) received the Ph.D. degree in telecommunications from the University of Trento, Italy, in 2014. He is currently an Associate Professor with Al-Hussein Bin Talal University, Jordan. He has authored more than 100 scientific articles. His research interests include a wide range of wireless communications topics, such as index modulation, physical-layer security, spectrum sharing, cognitive radio, wireless sensor networks, energy efficiency, non-orthogonal multiple access, the Internet of Things, and resource allocation. He is a member of IEEE ComSoc R8 Board. He served as a General Co-Chair for BROADNETs2018 Conference. He is also coordinating the Distinguished Lecturer Program in IEEE ComSoc R8.

KENTA UMEBAYASHI (Member, IEEE) received the L.L.B. degree from Ritsumeikan University, Japan, in 1996, and the B.E., M.E., and Ph.D. degrees from Yokohama National University, Japan, in 1999, 2001, and 2004, respectively. From 2004 to 2006, he was a Research Scientist with the Centre for Wireless Communications, University of Oulu, Finland. He is currently a Professor with Tokyo University of Agriculture and Technology, Japan. He was a Principal Investigator of four grants-in-aid for scientific research projects and three strategic information and communications research and development promotion program projects, including a HORIZON2020 Project. His research interests include signal detection and estimation theories for wireless communications, signal processing for multiple antenna systems, cognitive radio networks, and terahertz band wireless communications. He received the Best Paper Award at 2012 IEEE WCNC and the Best Paper Award at 2015 IEEE WCNC Workshop from IWSS.

NIZAR ZORBA (Senior Member, IEEE) is currently a Professor with the Electrical Engineering Department, Qatar University, Doha, Qatar. He has authored five international patents, two books, contributed to seven book chapters, and coauthored over 130 papers in peer-reviewed journals and international conferences. He is a Symposium Chair at IEEE GLOBECOM 2021, IEEE VTC 2020, and IEEE ICC 2019; a Workshop Chair at IEEE ICC 2021, IWCMC 2020, and CSM-PS 2019; and a Demo Chair at IEEE ISCC 2021. He is also the Chair of the IEEE ComSoc Communication Systems Integration and Modeling Technical Committee (TC CSIM). He is an Associate/Guest Editor of the IEEE Communications Letters, *IEEE IoT Magazine*, IEEE Access, *IEEE Communications Magazine*, and *IEEE Network*.